

Friction measurements on phase-separated thin films with a modified atomic force microscope

R. M. Overney*, E. Meyer*, J. Frommer*[‡],
D. Brodbeck*[‡], R. Lüthi*, L. Howald*,
H.-J. Güntherodt*, M. Fujihira[†],
H. Takano[†] & Y. Gotoh[†]

* Physics Institute, University of Basel, Klingelbergstrasse 82,
CH-4056 Basel, Switzerland

[†] Department of Biomolecular Engineering, Tokyo Institute of Technology,
Nagatsuta, Midori-ku, Yokohama 227, Japan

THE study of chemical phase separation in multicomponent thin organic films typically involves the addition of a dye which is selectively more soluble in one of the phases, thereby making it possible to probe the domain structures by fluorescence microscopy¹⁻⁴. The resolution of this approach is generally limited to tens of micrometres. The atomic force microscope, on the other hand, has recently proved useful for imaging organic thin films down to the atomic scale⁵⁻⁹, but this technique provides details of the overall film topography, rather than the chemical composition. Here we show that the recently developed friction force microscope¹⁰⁻¹³, which simultaneously measures both the normal and lateral forces on the scanning tip, can be used to image and identify compositional domains with a resolution of ~ 5 Å. Although the topography of the individual domains can be imaged with a standard atomic force microscope, it is the additional information provided by the friction measurement that allows them to be chemically differentiated.

Scanning probe microscopes such as the scanning tunnelling microscope¹⁴ (STM) and atomic force microscope⁵ (AFM) have been used to analyse surfaces on many levels, from molecular arrangements at interfaces to electronic structures in semiconductors⁹. These methods are rather insensitive to chemical composition; with the STM, electronic states around the Fermi energy are probed, whereas AFM images are interpreted as maps of the total charge density^{15,16}. Some elemental characterization has been possible with scanning tunnelling spectroscopy on samples such as GaAs¹⁷, adsorbates on semiconductors¹⁸ and metals¹⁹. For more detailed information, core levels have to be sensed, and this is not possible with the STM^{18,20}.

Frictional forces can influence AFM image contrast when it is operating in the repulsive contact mode^{10,11}. Those measurements show that frictional forces vary on an atomic scale and that a friction force coefficient for a tungsten tip on a graphite sample can be determined¹⁰. These observations led to the construction of a friction force microscope (FFM) where both the normal and lateral forces are measured simultaneously but separately over homogeneous surfaces¹¹⁻¹³. In this instrument, the bending and torsion of a cantilever-type spring are correlated with the normal and lateral forces exerted by the sample, while the fine resolution of an AFM is maintained. Here, we extend the use of the FFM to samples composed of distinctly different chemical species and demonstrate that the FFM can distinguish between these components.

From macroscopic measurements it is well known that friction depends strongly on material. Various types of apparatus have been used to measure frictional properties as a function of temperature, sliding velocity and normal load²¹⁻²³. The FFM represents a simplified device for experiments on sliding friction under boundary conditions: an idealized single asperity on a thin multilayer film. With the FFM the lateral (friction) forces acting on the probing tip can be measured over a localized

contact area of a few square nanometres between probing tip and sample.

To demonstrate that on the nanometre scale, frictional properties are sensitive to changes in surface properties on chemical modification^{24,25}, we have chosen Langmuir-Blodgett (LB) films because of their solid-like behaviour, their use in previous work on boundary lubrication²¹ and their well-defined, non-random structure²⁶, so that the results would be straightforward to interpret. But the FFM technique is applicable to a wide range of materials, for the study of material-specific friction and as a means of identifying materials on this very small scale from their different frictional responses. Few, if any, other techniques can probe material properties directly and nondestructively on so small a scale with such good resolution (~ 5 Å). Its usefulness has been demonstrated on layered materials such as mica¹² and graphite¹⁰. Here we demonstrate that the technique can be used to distinguish between components in a multicomponent system, as we assess not only the differential friction between two molecular classes (fluorocarbon and hydrocarbon), but also that between organic adsorbate and inorganic (silicon) substrate.

Figure 1a shows a $5.0 \times 5.0 \mu\text{m}^2$ top-view AFM image of a 50:50 molar mixture of arachidic acid and partially fluorinated carboxylic acid bound ionically to a common cationic polymer (see Fig. 2). Round island-like structures are observed, 100 nm to 1 μm in diameter and ~ 1.6 nm in height above the surrounding film. We assign the higher circular domains in Fig. 1a to the hydrocarbons and the surrounding flat film to the fluorocarbons, partly on the basis of their different molecular lengths and partly because of their different frictional behaviours (see below). With molecular lengths of ~ 2.5 nm and ~ 2.0 nm for the arachidic acid and the fluorocarbon-terminated acid,

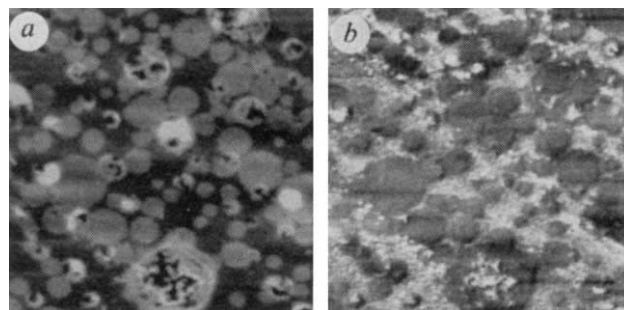


FIG. 1 The LB films are prepared as described elsewhere^{37,38}. Briefly, a 1:1 molar mixture of perhydro arachidic acid ($\text{C}_{19}\text{H}_{39}\text{COOH}$) and partially fluorinated carboxylic acid, ($\text{C}_9\text{F}_{19}\text{C}_2\text{H}_4\text{OC}_2\text{H}_4\text{COOH}$), is introduced in organic solvent to an aqueous subphase containing poly(4-vinyl-*N*-methylpyridinium) cationic polymer. The complex of anionic surfactants and cationic polymer is transferred by the LB technique onto a hydrophobized silicon (100) surface to form a bilayer system. Pretreatment of the silicon surface is explained elsewhere³⁹. The deposition of the LB films is carried out in a Langmuir trough at room temperature. The FFM cantilevers used here are microfabricated from Si_3N_4 and have normal and torsion spring constants of 0.2 N m^{-1} and 200 N m^{-1} , respectively. The resolution of the instrument is 0.1 Å in the normal direction and 10^{-10} N in the friction force. The measurements are done at minimal normal load, of the order of 10^{-9} - 10^{-8} N. **a**, AFM image ($5 \times 5 \mu\text{m}^2$) of the surface of a bilayer prepared from a mixture of the fluorocarbon and hydrocarbon carboxylates (1:1 molar). The image represents the topography. The circular domains are assigned to the hydrocarbon component and the surrounding flat film to the partially fluorinated component. The difference in height between these two regions is ~ 1.6 nm. Holes of ~ 5 nm in depth are observed only in the 'island-like' circular hydrocarbon domains, whereas the fluorinated film remains fairly uniform and unbroken. **b**, Friction force measurement (also covering $5 \times 5 \mu\text{m}^2$) done simultaneously with the topography image in **a**. The lateral force image indicates higher friction (brighter contrast) over the fluorinated regions. Highest friction is measured on the silicon surface (at the bottom of the holes in the film). No difference in contrast (friction) is observed between the hydrocarbon layers of different height.

[‡] Also at the IBM Almaden Research Center, San Jose, California 91520, USA.

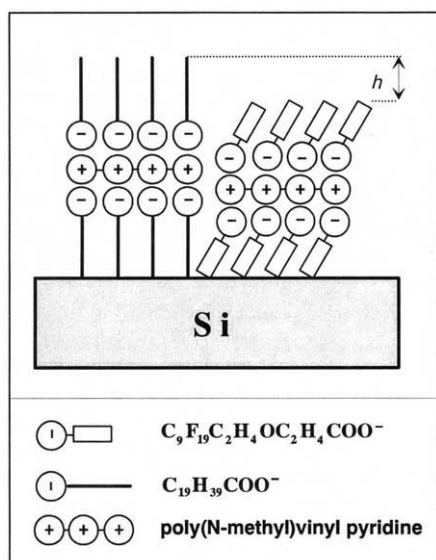


FIG. 2 Schematic view of the LB bilayer system imaged by AFM in Fig. 1. The 'h' represents the height difference between the hydrocarbon and fluorocarbon species (see text).

respectively, we expect a difference in height of ~ 1.0 nm between domains of the two components in this bilayer LB system. Figure 1a shows a step height from flat film to island of 1.6 nm; the slightly greater difference could be due to a greater tilt angle in the fluorocarbon domains²⁷.

In other experiments, AFM images have been recorded on LB bilayer films composed of a single carboxylic acid component, one from arachidate and one from the partially fluorinated carboxylate⁹. The fluorinated acid film contains fewer defects than the arachidic acid film⁹. These results support the assignment of the circular domains to the hydrocarbon component, as holes are observed only in the circular domains in the mixed films. These holes are ~ 5.0 nm in depth, consistent with the thickness of a bilayer. Furthermore, increasing the force while scanning disrupts the hydrocarbon but not the fluorinated areas, in both the one- and two-component films. The fluorinated sites show good resistance to rupture during sliding, in agreement with tribology experiments using macroscopic measurement techniques²³.

Lateral force measurements (Fig. 1b) made simultaneously with the topography measurements (Fig. 1a) indicate roughly four times higher friction over the fluorinated regions than over the hydrocarbon regions. Holes in the film reveal the silicon substrate. The silicon, appearing as dark (low) areas in the topography image, shows a friction force a factor of 10 higher than the hydrocarbon domains in the lateral force image. This difference in friction agrees well with other experiments on both macroscopic and nanometre scales²⁸⁻³⁰. In sum, from the FFM measurements on these phase-separated LB films, the relative frictions of the hydrocarbon, fluorocarbon and silicon surfaces are shown to be 1:4:10. In the range of nondestructive forces applied in this study, $\sim 10^{-9}$ – 10^{-8} N, no dependence of the friction on load is observed.

The differences in friction are not due to changes in topography. This is demonstrated particularly well by the ability of the friction measurements to identify the scattered islands of 'extraneous' material sitting atop hydrocarbon domains. Whereas normal force measurement determines only the geometry of the island, lateral force measurement determines its composition. The frictional response of the island corresponds to that of the circular hydrocarbon domains, thereby allowing it to be identified as hydrocarbon in nature. This assignment would not be possible with the normal AFM alone.

The friction on the fluorinated areas is higher than on the hydrocarbons. From the performance of fluorine-containing lubricants, such as teflon (PTFE), a reduction in friction might be expected. But it is known from surface force apparatus

experiments²³ that fluorinated LB films have larger shear strengths (friction force divided by the real area of contact in shear) than their hydrogen-containing counterparts. The higher friction measured with the FFM over the fluorocarbon is attributed, at least in part, to the greater stiffness and closer packing³¹ of the fluorocarbon moiety.

These observations of friction and robustness on the scale of nanometres can be applied to the study of tribology, particularly boundary lubrication. Boundary lubrication, as established by Hardy³², deals with the layers of lubricant closest to the solid surfaces undergoing frictional contact, and is of importance in most surface-on-surface sliding mechanisms. The particular advantage of the fluorinated film is its resistance to rupture as known from both the surface force apparatus and AFM measurements. The good performance of fluorocarbons as lubricants can therefore be attributed to high stability towards applied stress, and a reduced friction (compared with unlubricated surfaces) which reduces the wear to very low values (reduction of 10,000)³³.

In nanometre-scale friction and topography measurements, local elasticity plays a role. In our on-going work, we measure a greater elasticity on the molecular scale for the hydrocarbon moieties than the fluorocarbon moieties, evidence for the increased stiffness of fluorinated segments³¹. This is consistent with the higher in-plane cohesive binding that we observe in the fluorocarbon domains, also attributed to the higher barriers for *trans/gauche* isomerization in the stiffer fluorocarbon chains^{34,35}. Even though our observation of lower friction on the hydrocarbon film suggests that hydrocarbon acids could be more effective lubricants than the fluorinated compounds, our comparative measurements show that pure arachidate films and domains are more disrupted by sliding friction than their fluorocarbon counterparts^{9,36}. We propose that a good lubricating mixture would have a fluorinated component to offer good rupture resistance and a hydrocarbon component to contribute low friction, as in the mixture used here. □

Received 6 April; accepted 28 July 1992.

- Knobler, C. *J. Phys.: Condens. Matter* **3**, S17–S22 (1991).
- Möbius, D. & Möhald, H. *Adv. Mater.* **3**, 19–24 (1991).
- Seul, M. & Sammon, M. *J. Phys. Rev. Lett.* **64**, 1903–1906 (1990).
- Chi, L. F., Johnston, R. R. & Ringsdorf, H. *Langmuir* **7**, 2323–2329 (1991).
- Binnig, G., Quate, C. F. & Gerber, C. *Phys. Rev. Lett.* **56**, 930–933 (1986).
- Meyer, E. *et al. Nature* **349**, 398–400 (1991).
- Bourdieu, L., Silberzan, P. & Chatenay, D. *Phys. Rev. Lett.* **67**, 2029–2031 (1991).
- Alves, C., Smith, E. & Porter, M. *J. Am. Chem. Soc.* **114**, 1222–1227 (1992).
- Frommer, J. *Angew. Chem.* **31** (in the press).
- Mate, C. M., McClelland, G. M., Erlandsson, R. & Chiang, S. *Phys. Rev. Lett.* **59**, 1942–1945 (1987).
- Meyer, G. & Amer, N. M. *Appl. Phys. Lett.* **57**, 2089–2091 (1990).

12. Marti, O., Colchero, J. & Mlynek, J. *Nanotechnology* **1**, 141–144 (1990).
13. Eriandsson, R. *et al. J. Chem. Phys.* **89**, 5190–5193 (1988).
14. Binnig, G., Rohrer, H., Gerber, C. & Weibel, E. *Appl. Phys. Lett.* **40**, 178–181 (1982).
15. Binnig, G. *et al. Europhys. Lett.* **3**, 1281–1286 (1987).
16. Meyer, E. *et al. J. Vac. Sci. Technol.* **B2**, 1329–1332 (1991).
17. Feenstra, R. M., Strosio, J. A., Tersoff, J. & Fein, A. P. *Phys. Rev. Lett.* **58**, 1192–1195 (1987).
18. Hamers, R. J., Avouris, Ph. & Bozso, F. *J. Vac. Sci. Technol.* **A6**, 508–511 (1988).
19. Behm, R. J. *Scanning Tunneling Microscopy and Related Methods* (eds Behm, R. J., Garcia, N. & Rohrer, H.) 173–209 (NATO ASI Series, 1990).
20. Feenstra, R. M. *Scanning Tunneling Microscopy and Related Methods* (eds Behm, R. J., Garcia, N. & Rohrer, H.) 211–240 (NATO ASI Series, 1990).
21. Bowden, F. P. & Tabor, D. *The Friction and Wear of Solids* (Oxford Univ. Press, London, 1950).
22. Israelachvili, J. N. & Tabor, D. *Wear* **24**, 386–390 (1973).
23. Briscoe, B. J. & Evans, D. C. B. *Proc. R. Soc. A* **380**, 389–407 (1982).
24. Murray, R. W. *Electroanalytical Chemistry*, Vol. 13 (ed. Bard, A. J.) 191–368 (Dekker, Marcel, New York, 1984).
25. Fujihira, M. *Topics in Organic Electrochemistry* (eds Fry, A. J. & Britton, W. E.) 255–294 (Plenum, New York, 1986).
26. Ullman, A. *An Introduction to Ultrathin Organic Films from Langmuir–Blodgett to Self-Assembly* (Academic, New York, 1991).
27. Naselli, C., Swalen, J. D. & Rabolt, J. F. *J. chem. Phys.* **90**, 3855–3860 (1989).
28. Briscoe, B. & Tabor, D. *Interfacial Phenomena in Apolar Media* (eds Eicke, H.-F. & Parfitt, G. D.) 327–356 (Dekker, Marcel, New York, 1987).
29. Meyer, E. *et al. Fundamentals of Friction* (eds Pollock, M. & Singer, I.) (Kluwer, in the press).
30. Meyer, E. *et al. Ultramicroscopy* (in the press).
31. Barton, S. W. *et al. J. chem. Phys.* **96**, 1343–1351 (1992).
32. Hardy, W. B. *Proc. R. Soc. A* **88**, 313–315 (1913).
33. Rabinowitz, E. & Tabor, D. *Proc. R. Soc. A* **208**, 455–474 (1951).
34. Hsu, S. L. *et al. Macromolecules* **23**, 4565 (1990).
35. Bates, T. W. & Stockmayer, W. H. *Macromolecules* **1**, 12 (1968).
36. Meyer, E. *et al. Thin Solid Films* (in the press).
37. Umemura, J. *et al. Thin Solid Films* **178**, 281 (1989).
38. Nishiyama, K., Kurihara, M. & Fujihira, M. *Thin Solid Films* **179**, 477 (1989).
39. Schreck, M. *et al. Thin Solid Films* **175**, 95–105 (1989).

ACKNOWLEDGEMENTS. The work in Switzerland was supported by the Swiss National Science Foundation, the Kommission zur Förderung der wissenschaftlichen Forschung. The work in Japan was supported by the Ministry of Education, Science, and Culture and by the Nissan Science Foundation.

Increased ultraviolet radiation in New Zealand (45° S) relative to Germany (48° N)

G. Seckmeyer*‡ & R. L. McKenzie†‡

* GSF, Institut für Biochemische Pflanzenpathologie, Inglostädter Landstrasse 1, D-8042 Neuherberg, Germany

† DSIR Physical Sciences, Lauder 9182, Central Otago, New Zealand

RECENT analyses of global ozone measurements have confirmed that ozone reductions are not confined to the Antarctic, but now extend to mid-latitudes in both hemispheres^{1,2}. Ozone reductions lead to increases in biologically damaging ultraviolet radiation³, and such increases have been observed in Antarctica^{1,4} and Australia⁵. Little is known, however, about hemispheric differences in ultraviolet intensities. Here we use a combination of spectral measurements made in Germany and New Zealand with the same spectroradiometer, together with model calculations, to show that in the New Zealand summer of 1990–1991 biologically weighted ultraviolet irradiances were nearly a factor of two greater than those in the summer at similar northern latitudes in Germany. These differences are larger than expected^{3,6}, and are due mainly to decreased stratospheric ozone over New Zealand and increased levels of tropospheric ozone over Germany.

The instrumentation⁷ comprises a horizontal cosine-response diffuser coupled by a quartz fibre optic and an optical chopper to a 0.3-m double monochromator with spectral resolution 1 nm. A photomultiplier detector is used, and data acquisition over the spectral range 290–410 nm is computer-controlled. The scan duration is typically 5 minutes, depending on the light levels. We used the same instrument (temperature-stabilized to 20.0 ± 0.5 °C), method and calibration standards for all measurements, thus avoiding the problem of instrument intercalibration.

‡ Address for G.S. from 1 October: Fraunhofer-Institut für Atmosphärische Umweltforschung (IFU), Kreuzteckbahnstrasse 19, 8100 Garmisch-Partenkirchen, Germany. Present address for R.L.M.: National Institute of Water and Atmospheric Research Ltd, Te Tari Taihoro Nukurangi (NIWAR), Atmospheric Division, Lauder, Private Bag, Omakau, New Zealand.

Ideally, any comparison should cover an extended period, with continuous observations over a wide range of solar elevations and weather conditions. This has not yet been possible, and here we investigate clear-sky irradiances only. Before the New Zealand campaign, measurements were made at Neuherberg (48.2° N, 11.5° E, altitude 500 m) and the Wank Mountain (47.5° N, 11.1° E, 1,800 m) in Southern Germany in short campaigns since 1986. In New Zealand, data were obtained continuously over daylight hours at Lauder (45° S, 170° E, 300 m) in the summer between mid-November 1990 and mid-March 1991. Data before February were not useful, however, because of calibration difficulties. Good-quality clear-sky data were available only on 21 and 28 February, and 6, 7, 9 and 10 March. Subsequently, data were taken at Neuherberg on 13 July 1990 and on selected days between 26 July and 13 September 1991 (clear skies 29, 30 July). Ozone column measurements from a Dobson spectrophotometer, and profiles measured with balloonsondes, were available at Lauder and Hohenpeissenberg (60 km southwest of Neuherberg). Figure 1 gives an example of the clear-sky ultraviolet irradiances measured at 1 nm spectral resolution and for the same solar zenith angle (34.3°) in Neuherberg and Lauder: the Lauder irradiance at 300 nm (strong ozone absorption) is 2.72 times as great as in Germany, but at 330 nm (weak absorption by ozone) it is only 1.05 times as great. These large differences are mainly due to the difference of 86 Dobson units (DU) in total column ozone. A calculation of differences for average conditions is given later. The spectra were multiplied by two biological weighting functions that represent the relative damaging effect for DNA⁸ and for human skin (erythema)⁹. The weighted irradiance measurements were, respectively, 1.9 and 1.6 times as large at Lauder as at Neuherberg, mainly because of the lower ozone amounts at Lauder.

To investigate whether the irradiance differences were typical for the summer, we compared measured and modelled irradiances. Ozone column measurements were used to calculate ultraviolet spectra, using an adaptation of a simple parametric clear-sky radiative transfer model known as the 'Green model'^{10,11}. Input parameters for the model are: extraterrestrial irradiance, Sun elevation angle, ozone column, height above sea level, albedo, turbidity parameter (aerosol optical depth) and air pressure. The adaptation includes the use of a solar reference spectrum^{12,13} convolved with the instrument slit function. All the clear-sky measurements showed good agreement with calculated spectra (Fig. 2). Although there are wavelength-dependent differences of up to 40%, the biologically weighted irradiances agree to within 5–10%. The measured and calculated irradiances in Neuherberg show similar agreement when ozone values (from Hohenpeissenberg) are reduced by 3%. Results from a recent

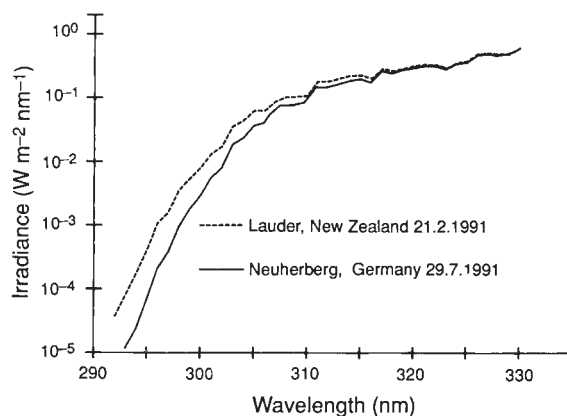


FIG. 1 Measured spectral irradiance in New Zealand and Germany for two summer conditions for solar zenith angle 34.3°. The ozone column was 266 DU in New Zealand and 352 DU in Germany (1 DU = 2.69 × 10¹⁶ molecule cm⁻²).